J. Biophotonics **4**, No. 10, 696–706 (2011) / **DOI** 10.1002/jbio.201100037

Journal of BIOPHOTONICS

FULL ARTICLE

Comparative evaluation of the diagnostic performance of autofluorescence and diffuse reflectance in oral cancer detection: a clinical study

Jayaraj L. Jayanthi[1], *Narayanan Subhash*[*,1], *Manju Stephen*[2], *Emmanuel K. Philip*[2], *and Valappil T. Beena*[2]

[1] Biophotonics Laboratory, Centre for Earth Science Studies, Akkulam, Trivandrum, India
[2] Department of Oral & Maxillofacial Pathology, Government Dental College, Trivandrum, India

Received 9 May 2011, revised 28 July 2011, accepted 22 August 2011
Published online 12 September 2011

Key words: Tissue autofluorescence, diffuse reflectance spectroscopy, principal component analysis, linear discriminant analysis, ROC curve, oral cancer

Autofluorescence (AF) and diffuse reflectance (DR) spectroscopic techniques have shown good diagnostic accuracies for noninvasive detection of oral cavity cancer. In the present study, AF and DR spectra recorded in vivo from the same set of sites in 65 patients were analyzed using Principal component analysis (PCA) and linear discriminant analysis (LDA). The effectiveness of these two techniques was assessed by comparison with gold standard and their discrimination efficiency was determined from the area under the receiver operator characteristic (AUC-ROC) curve. Analysis using a DR technique shows a higher AUC-ROC of 0.991 as against 0.987 for AF spectral data.

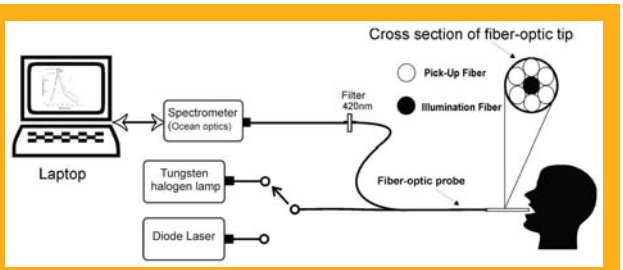

Schematic of the LIFRS point monitoring setup.

1. Introduction

Oral cancer represents a significant health problem owing to its high rate of incidence in India as well as the world over. Squamous cell carcinoma (SCC) contributes to around 85% of oral malignancies. It appears as leukoplakia or erythroplakia with their chances of conversion to malignancy being approximately 10% and 90%, respectively [1]. The chances of survival of patients with oral cavity carcinoma are markedly improved through early detection and treatment. Current diagnostic methods for superficial cancers rely on visual inspection of lesions, which is subjective, followed by biopsy from the most malignant site identified by visual inspection. Such procedures are invasive, and diagnosis often requires a waiting period of several days to weeks. Since identification of a suspicious area is based only on visual examination, a significant number of false-positive cases also undergo biopsy. It is possible that an oral lesion that is premalignant at some part may not be malignant at another location. Therefore, biopsy from one location of a lesion cannot be representative of the entire lesion and many malignant

* Corresponding author: e-mail: subhashnarayanan@gmail.com, Tel.: 91-471-2511638, Fax: 91-471-2442280

lesions also get overlooked [2]. Biopsy of large lesions often requires multiple biopsies that lead to substantial tissue removal. Though this protocol is accepted as the gold standard, it is invasive and time consuming. Also, the resemblances of tissue inflammation and irritation with premalignant oral mucosal alterations and field cancerous changes are often challenging. This usually leads to random or repeated biopsies causing great discomfort to the patient.

An optical instrument for tissue diagnosis should ideally provide high diagnostic accuracy combined with information on the structure and function of tissue. The prevalence of various optical spectroscopy techniques has been increasing in the biomedical field and is getting greater recognition and acceptance these days owing to their ability for noninvasive tissue characterization. The advantage of optical techniques over other methodologies is that they provide quantitative information that can be analyzed instantaneously and produce an objective diagnosis even in the hands of a less-skilled operator.

Optical spectroscopy is an evolving technique with high diagnostic potential because of its ability to detect biochemical and morphological changes that occur in tissue during neoplastic progression. Cellular and architectural changes, linked to dysplastic progression in epithelial tissue, affect the absorption, scattering and fluorescence properties of tissue, and lead to diagnostically significant differences in clinically measured spectra. Methods of optical spectroscopy and imaging are being developed by various research groups for a variety of biomedical applications in non- or minimally invasive tissue diagnostics, including sensing of molecular concentrations of delivered pharmaceutical or contrast agents, probing tissue physiologic status, and detecting early stage of diseases in vitro and in vivo [1, 3–7].

A number of studies have explored the utility of diffuse reflectance (DR) and autofluorescence (AF) spectroscopy for the detection of cancerous lesions in various organs [3, 8–13]. De Veld et al. has given an extensive review of AF and DR in oral oncology [4]. Mourant et al. [8] used reflectance spectroscopy to distinguish malignant sites from nonmalignant sites in the bladder with a sensitivity of 100% and a specificity of 97%. Zhu and Palmer [9] obtained a sensitivity and specificity of 80% for discriminating malignant and nonmalignant breast tissues using the Monte Carlo inverse model with a PCA algorithm. The DR spectral ratio (R545/R575) was used by Mallia et al. [10] in a clinical trial to discriminate precancerous dysplastic lesions from hyperplastic tissue with a sensitivity of 100% and a specificity of 86%. Ramanujam et al. [11] combined principal component analysis (PCA) and logistic regression for classification of human cervical tissue fluorescence in vivo and reported an overall sensitivity of 88% and specificity of 70% to differentiate squamous intraepithelial lesions (SILs) from normal squamous epithelia and inflammation. Using partial least squares (PLS) and artificial neural network (ANN)-based classification model, Wang et al. [12] obtained a sensitivity of 81% for recognizing premalignant and malignant tissues and a specificity of 96% for identifying benign samples that consists of normal, oral submucous fibrosis and epithelial hyperplasia. Kamath and Mahato [13] discussed the potential of fluorescence spectroscopy for detection of oral carcinomas in vitro by classification of the spectra by PCA and *k*-means nearest-neighbor analysis and obtained a specificity, sensitivity and accuracy of 100%, 94.5% and 96.2%, respectively.

In this clinical trial, we record the AF and DR spectra from the same set of oral cavity lesions in 65 patients and compare the efficacy of these two optical biopsy techniques by correlating the results with histopathological reports. The data was analyzed using PCA and linear discriminant analysis (LDA) to examine the potential utility of these optical biopsy techniques and the results are presented.

2. Materials and methods

2.1 Study population and study settings

The study population consisted of a total of 30 healthy volunteers maintaining good oral hygiene and without any inflammations/visible lesions in the oral cavity, selected by a dental pathologist and 65 patients registered in the outpatient clinic of the Government Dental College (GDC), Trivandrum, who have volunteered to participate in this trial. Before enrollment, the study subjects were examined for suspicious lesions such as white/red patches, nonhealing ulcers, ulcero-proliferative growth and erosive lichenplanus in their oral cavity. Informed consent was obtained from all the patients involved in the study and the protocol was approved by the Ethics Committee of GDC (approval number: IEC/C/28-A/2010/DCT).

2.2 Instrumentation

The laser-induced fluorescence and reflectance spectroscopy (LIFRS) system consists of two light sources that could be alternatively switched on/off for sequential recording of tissue AF and DR spectra (Figure 1). White light from a tungsten-halogen lamp (Ocean Optics, Dunedin, Florida, USA, Model: LS-1-LL,) is used to record the DR spectrum, whereas

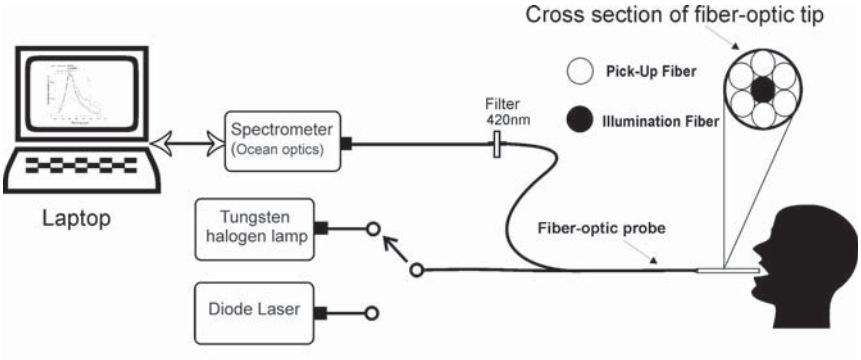

Figure 1 Schematic of the LIFRS point monitoring setup used in the clinical trial.

the fluorescence measurements were performed with excitation at 404 nm from a diode laser (Deal Extreme, China, 50 mW, CW). A bifurcated optical fiber guides the light emission from either of these two sources to the lesion through a fiber-optic reflection probe that has a 3-m long central fiber to deliver the excitation beam and six surrounding fibers (each of 400 μm diameter) to collect tissue DR and AF. The reflection probe tip is terminated in a stainless-steel ferrule of 15 cm length and 6 mm diameter for easy access to the oral cavity and to enable sterilization before and after use. A black PVC disposable sleeve of length 10 mm inserted at the probe tip provides extra hygiene and maintains a fixed separation of approximately 3.5 mm between the probe tip and the tissue for maximizing the optical signal by providing optimal overlap between the excitation and collection areas. The light collected from the sample is delivered to a miniature fiber-optic spectrometer (Ocean Optics, Dunedin, Florida, USA, Model: USB 2000FL VIS-NIR), connected to the USB port of a laptop computer. During fluorescence studies, a long-wavelength pass filter (Schott: GG420) is inserted in the collection path for blocking the scattered laser light from entering the spectrometer. The LIAF and DR spectra are acquired in the 420–720 nm spectral range with the help of the OOI Base32 software (supplied by Ocean Optics) which is configured to record the spectra, averaged for 40 scans, with a boxcar width of 8 nm and an integration time of 100 ms.

2.3 Data acquisition/protocol

The suspicious lesions were visually identified and spectral measurements were taken from the selected sites of all patients using the point monitoring system described (Figure 1). Lesions from the buccal mucosa, palate, ventral tongue and floor of the mouth were included in this study while those on the dorsal/lateral sides of the tongue and the vermilion border of the lip were excluded as bacteria present in these sites emit fluorescence at 635 nm that interferes with the protoporphyrin IX fluorescence [14, 15]. Before measurements, all patients and healthy volunteers were asked to rinse their mouth with 0.9% saline solution for two minutes in order to reduce the effect of recently consumed food. They were also provided with protective goggles to shield their eyes against laser light. Fifteen sets of spectral measurements were taken from each site, probing circularly from the center of the lesion to the border, covering an area of ~6 mm diameter. Afterwards, an incisional biopsy (2×2 mm approximately in size) was taken from the site that showed most malignant changes during optical probing. The biopsy slides were prepared and classified by an experienced pathologist who was blinded to the spectral results. In the case of healthy volunteers, visual impression was carried out instead of biopsy. After recording of AF and DR spectra the results were analyzed and correlated with histopathological findings.

2.4 Statistical analysis

The AF and DR spectral data were normalized to the peak intensity to avoid interpatient and intrapatient variations. PCA and LDA were performed over the fluorescence and reflectance spectral data [16, 17]. PCA was used to identify the orthogonal components of the spectra with maximum variance within the complete data set. Significant PCs were identified using analysis of variance (ANOVA) and retained for further analysis. LDA was then performed on the extracted significant principal components and a discriminant function based on linear combinations of the input variables that provide the maximum discrimination between the groups was generated. Diagnostic accuracies were assessed from the scatter plot of the discriminant functions by comparison with histopathological results.

3. Results

The study population of 65 patients consisted of 15 cases of hyperplasia with no dysplasia, 24 cases of SCCs cover well, moderately and poorly differentiated categories and 26 cases of dysplasia that included mild, moderate and severe dysplasias. Spectral characteristics of the lesions studied, their visual impression, and pathological results are given in Table 1.

Table 1 Spectroscopic study results in patients with their clinical and histopathological reports.

Clinical description	Biopsy report	Point monitoring	
		AF	DR
Buccal Mucosa:			
1. Erythroplakia	Severe dysplasia/CIS	dysplasia	dysplasia
2. Ca	WDSCC	SCC	SCC
3. Erosive LP	Erosive LP	SCC	SCC
4. Leukoplakia	EHP with Mild dysplasia	dysplasia	Dysplasia
5. Leukoplakia	Moderate dysplasia	dysplasia	Dysplasia
6. Ulcero proliferative	MDSCC	SCC	SCC
7. Ulcero proliferative	MDSCC	SCC	SCC
8. Ulcero proliferative	WDSCC	SCC	SCC
9. Leukoplakia	EHP with mild dysplasia	dysplasia	dysplasia
10. Ulcero proliferative	WDSCC	SCC	SCC
11. Ca	WDSCC	SCC	SCC
12. Erythroleukoplakia	EHP with mild dysplasia	dysplasia	dysplasia
13. Lichenplanus	Lichenplanus	hyperplasia	hyperplasia
14. Leukoplakia	WDSCC	SCC	SCC
15. Speckled leukoplakia	Moderate dysplasia	dysplasia	dysplasia
16. Leukoplakia	EHP with no dysplasia	hyperplasia	hyperplasia
17. Traumatic ulcer	No dysplasia	hyperplasia	hyperplasia
18. Ulcerated lesion	EHP with no dysplasia	hyperplasia	hyperplasia
19. Leukoplakia	EHP with no dysplasia	hyperplasia	hyperplasia
20. Leukoplakia	EHP with no dysplasia	hyperplasia	hyperplasia
21. Leukoplakia	Moderate dysplasia	dysplasia	Dysplasia
22. Ulcero proliferative	MDSCC	dysplasia	SCC
23. Ulcero proliferative	Moderate dysplasia	dysplasia	dysplasia
24. Leukoplakia	EHP with mild dysplasia	hyperplasia	dysplasia
25. Ulcero proliferative	WDSCC	dysplasia	dysplasia
26. Leukoplakia	Moderate dysplasia	dysplasia	dysplasia
27. Erythroleukoplakia	EHP with mild dysplasia	dysplasia	dysplasia
28. Lichenplanus	lichenplanus	hyperplasia	hyperplasia
29. Leukoplakia	WDSCC	SCC	SCC
30. Erythro leukoplakia	Severe dysplasia	hyperplasia	dysplasia
31. Leukoplakia	EHP with no dysplasia	hyperplasia	dysplasia
32. Traumatic ulcer	Severe dysplasia	SCC	dysplasia
33. Ulcerated lesion	EHP with no dysplasia	hyperplasia	hyperplasia
34. Leukoplakia	EHP with no dysplasia	hyperplasia	hyperplasia
Floor of the Mouth:			
35. Ca	PDSCC	SCC	SCC
36. Leukoplakia	No dysplasia	hyperplasia	hyperplasia
37. Leukoplakia	EHP with mild dysplasia	dysplasia	dysplasia
38. Ulcero proliferative	Moderate dysplasia	dysplasia	Dysplasia
39. Leukoplakia	minimal dysplasia	dysplasia	dysplasia
40. Leukoplakia	EHP with no dysplasia	hyperplasia	hyperplasia
41. Leukoplakia	Mild dysplasia	dysplasia	dysplasia
42. Leukoplakia	EHP with no dysplasia	hyperplasia	hyperplasia
43. Ca	WDSCC	SCC	SCC
44. Ca	Severe dysplasia	SCC	dysplasia
45. Leukoplakia	Moderate dysplasia	dysplasia	dysplasia
46. Ca	WDSCC	dysplasia	SCC

Table 1 continued

Clinical description	Biopsy report	Point monitoring	
		AF	DR
Ventral tongue:			
47. leukoplakia	Mild dysplasia	dysplasia	dysplasia
48. Ca	WDSCC	SCC	SCC
49. Ca	MDSCC	SCC	SCC
50. Verrucous growth	Mild dysplasia	dysplasia	dysplasia
51. Ca	WDSCC	SCC	SCC
52. leukoplakia	EHP with no dysplasia	hyperplasia	hyperplasia
53. Verrucous growth	MDSCC	SCC	SCC
54. leukoplakia	Minimal dysplasia	dysplasia	dysplasia
Commissure:			
55. leukoplakia	Moderate dysplasia	dysplasia	dysplasia
56. Ca	WDSCC	SCC	SCC
57. Ca	MDSCC	SCC	SCC
58. leukoplakia	MDSCC	SCC	SCC
Palate:			
59. leukoplakia	EHP with Mild dysplasia	dysplasia	Dysplasia
60. Ulcero proliferative	MDSCC	SCC	SCC
Alveolus:			
61. Ca	MDSCC	SCC	SCC
62. leukoplakia	EHP with no dysplasia	hyperplasia	hyperplasia
63. Ca	MDSCC	SCC	SCC
64. Ca	WDSCC	SCC	SCC
65. leukoplakia	EHP with no dysplasia	hyperplasia	hyperplasia

WDSCC – well differentiated squamous cell carcinoma, MDSCC – moderately differentiated squamous cell carcinoma, EHP – Epithelial Hyperplasia, LP – Lichen planus, CIS – carcinoma-in-situ, AF – Fluorescence, DR – diffuse reflectance, Ca – Carcinoma

3.1 Spectral features

The normalized AF spectra of normal, hyperplastic, dysplastic and SCC lesions from the buccal mucosa, floor of the mouth and ventral side of the tongue are given in Figures 2a, 3a and 4a, respectively. The AF spectra show strong emission around 500 nm in all cases, while dysplastic and SCC lesions show two additional peaks at 635 and 685 nm. A redshift is also noticed for the 500 nm band when the tissue becomes malignant. This peak has been reported as due to emission from endogenous fluorophores like NADH, FAD, collagen, elastin and amino acids, while the 635 and 705 nm peaks are from enhanced occurrence of PpIX in malignant tissues. The additional peak seen at 685 nm in SCC and dysplastic lesions could be due to the accumulation of corproporphyrin III, a constituent of the heme synthesis pathway in malignant tissues [14].

The DR spectra from normal, hyperplastic, dysplastic and SCC lesions showed significant dips around 545 and 575 nm (Figures 2b, 3b and 4b). The oxygenated hemoglobin absorption dips are more prominent in normal and hyperplastic/benign lesions as compared to tissues with abnormality. Further, a reduction in spectral intensity was noticed as the stage of malignancy increases.

3.2 Lesion classification

AF and DR spectral data gathered using LIFRS is used in lesion classification based on the discriminant function generated by LDA on significant PCs.

3.2.1 AF spectral data

PCA performed over the fluorescence spectral data extracts five PCs that account for 99.3% of the total variance of spectral data (PC1: 54%, PC2: 40%, PC3: 3.2%, PC4: 1.3%, and PC5: 0.45%). PC1, PC2 and PC4 were found to be statistically significant across various lesion groups (P value < 0.005) using ANOVA. These significant PCs were considered as

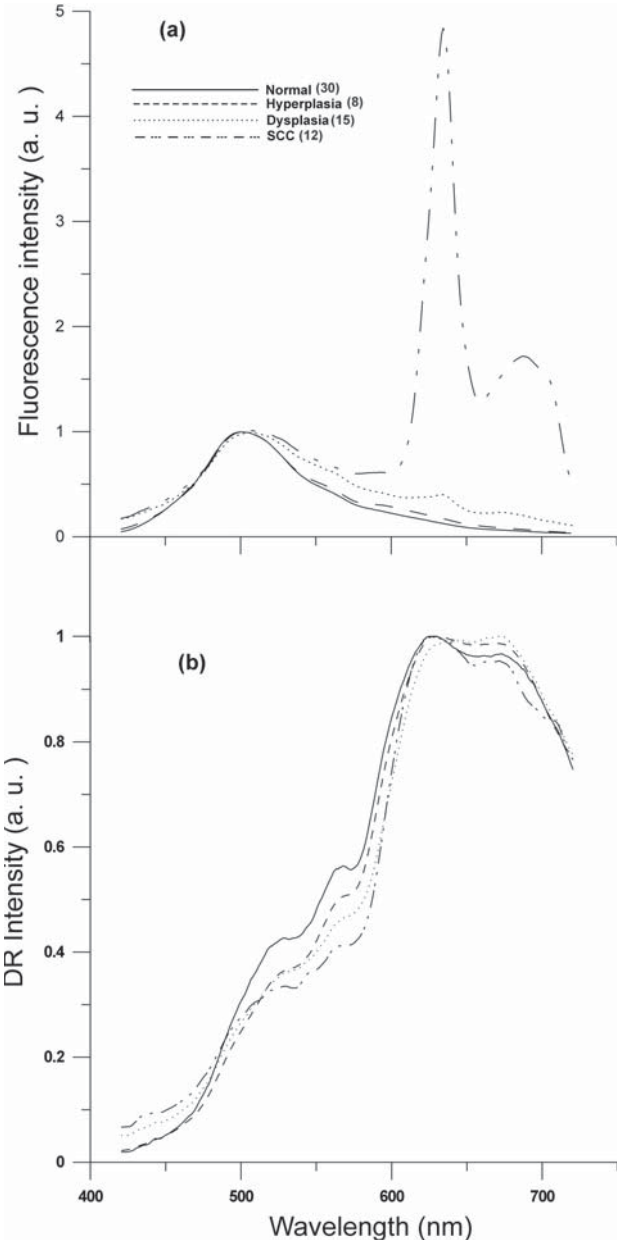

Figure 2 Spectral features of the buccal mucosa (BM) categorized as normal, hyperplasia, dysplasia and SCC; (**a**) averaged fluorescence emission normalized to the emission intensity at 500 nm, and (**b**) averaged DR spectra normalized to the peak intensity. Number of subjects examined under each category is given in parenthesis.

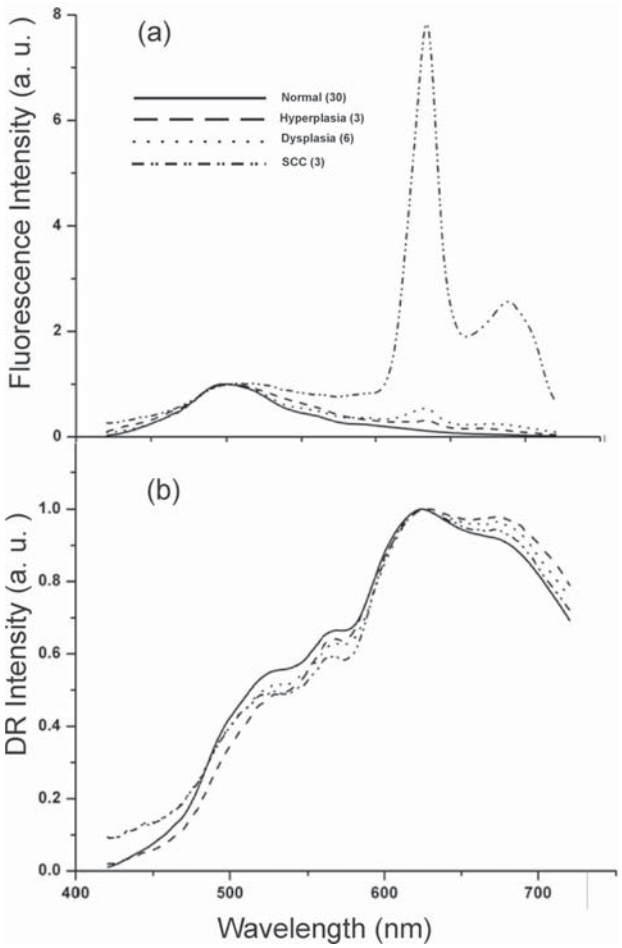

Figure 3 Spectral features of lesions in the floor of the mouth (FM) categorized as normal, hyperplasia, dysplasia and SCC; (**a**) averaged fluorescence emission normalized to the emission intensity at 500 nm, and (**b**) averaged DR spectra normalized to the peak intensity at 620 nm. Number of subjects examined under each category is given in parenthesis.

the input variables for LDA. A scatter plot of discriminant function (DF) scores (Figure 5) for normal and hyperplasia lesions shows that out of the 30 cases of healthy/normal lesions the study procedure has misclassified only two normal tissues as hyperplasia. Further, for discriminating hyperplasia from dysplasia specificity of 100% and sensitivity of 92% were obtained, where only two out of 26 dysplastic cases were misclassified. In comparison, for discriminating SCC from dysplasia, two out of 26 dysplasia cases were misclassified as SCC and one out of the 24 SCC cases was misclassified. Thus, sensitivities of 100%, 92% and 96%, and specificities of 93%, 100% and 92%, respectively, were obtained for discriminating hyperplasia from normal, dysplasia from hyperplasia and dysplasia from SCC (Table 2).

3.2.2 DR spectral data

PCA of the DR spectral data extracts six PCs that account for 99.6% of the variance in the entire spectral data (PC1: 34.5%, PC2: 32%, PC3: 15.9%, PC4: 11%, PC5: 5%, PC6: 1%). PC1, PC2, PC4,

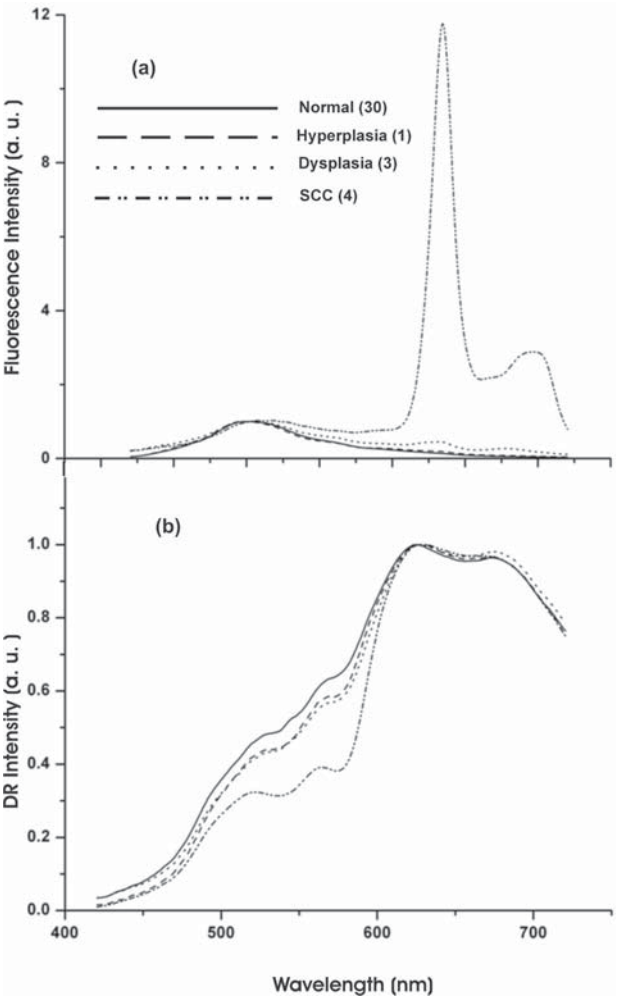

Figure 4 Spectral features of lesions in the ventral side of the tongue (VT) categorized as normal, hyperplasia, dysplasia and SCC; (**a**) averaged fluorescence emission normalized to the emission intensity at 500 nm, and (**b**) averaged DR spectra normalized to the peak intensity at 620 nm. Number of subjects examined under each category is given in parenthesis.

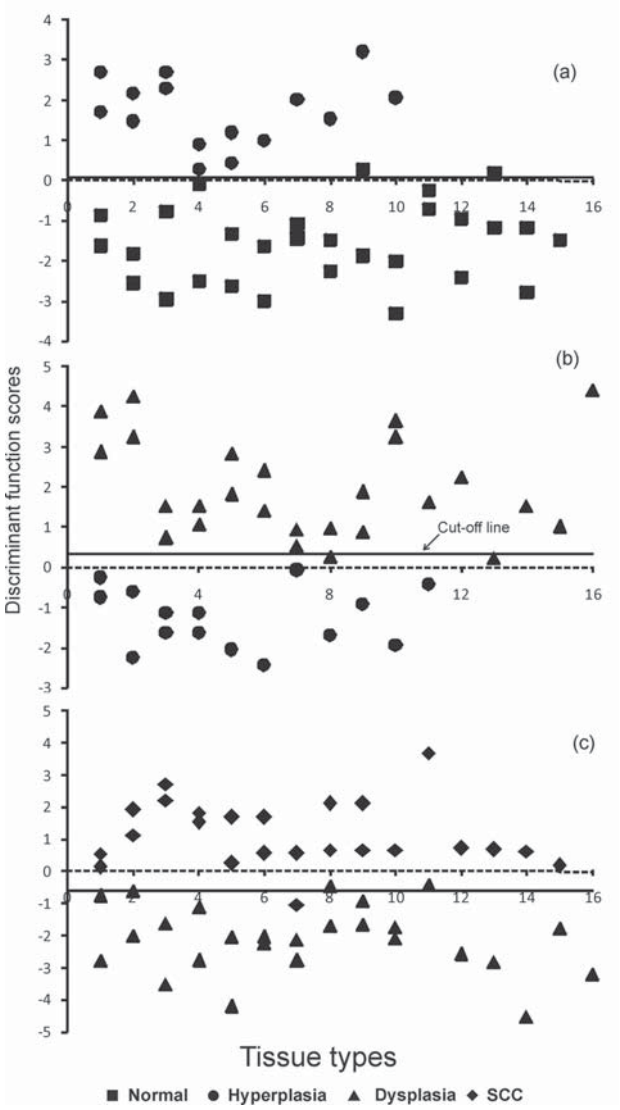

Figure 5 Discriminant function scatterplot of different lesion pairs for fluorescence spectral data, (**a**) normal – hyperplasia, (**b**) hyperplasia – dysplasia, and (**c**) dysplasia – SCC. The continuous line represents the cut-off value in each pair.

PC5 and PC6 were found to be significant (P value < 0.005) by ANOVA and were considered as the input variables for LDA. In comparison, the DF scatter plot of DR spectral data (Figure 6) yielded 100% diagnostic accuracy for discriminating normal from hyperplasia. Sensitivity of 100% and specificity of 93% were obtained for the discrimination of dysplasia from hyperplasia, where all the dysplastic lesions were classified correctly with one case of hyperplasia getting misclassified. During discrimination of SCC lesions from dysplasia, all cases with SCC were classified correctly while one case out of 26 dysplasia cases was misclassified as SCC, thus achieving a sensitivity of 100% and specificity of 96% (Table 2).

The ROC analysis with discriminant score yielded area under the curve (AUC) of 0.987 for fluorescence spectral data and 0.991 for DR spectral data in discriminating oral cavity lesions (Figures 7a and b).

4. Discussion

The overall reduction in fluorescence spectral intensity in the blue-green region of dysplastic and cancerous oral lesions as compared to normal tissues from buccal mucosa (BM) (Figure 2a), floor of the

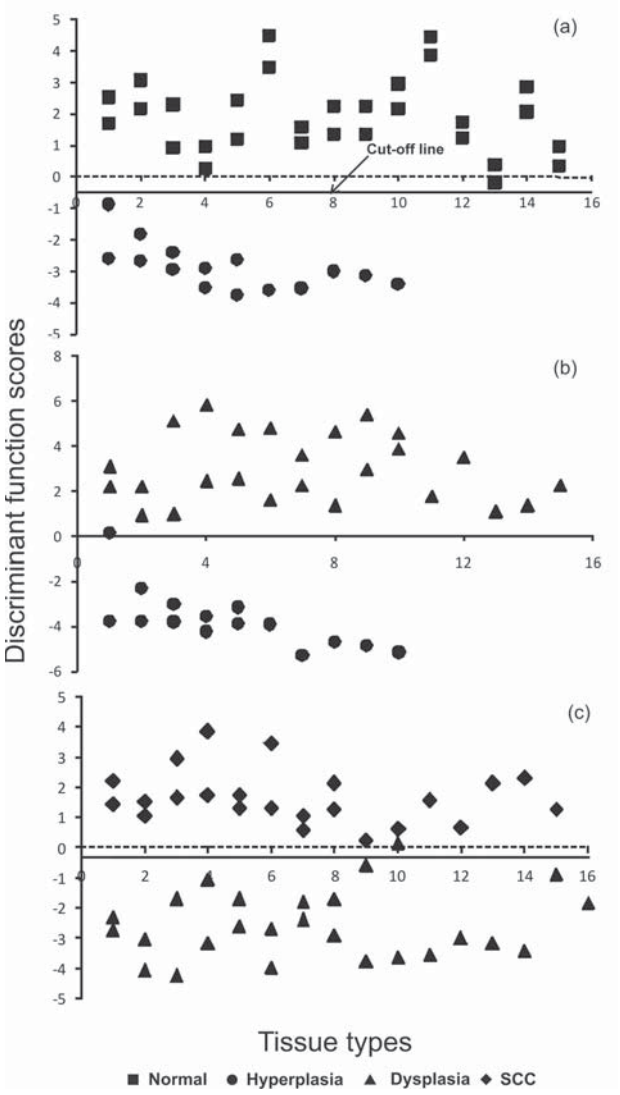

Figure 6 Discriminant function scatterplot of different lesion pairs for DR data, (**a**) normal – hyperplasia, (**b**) hyperplasia – displasia, and (**c**) dysplasia – SCC.

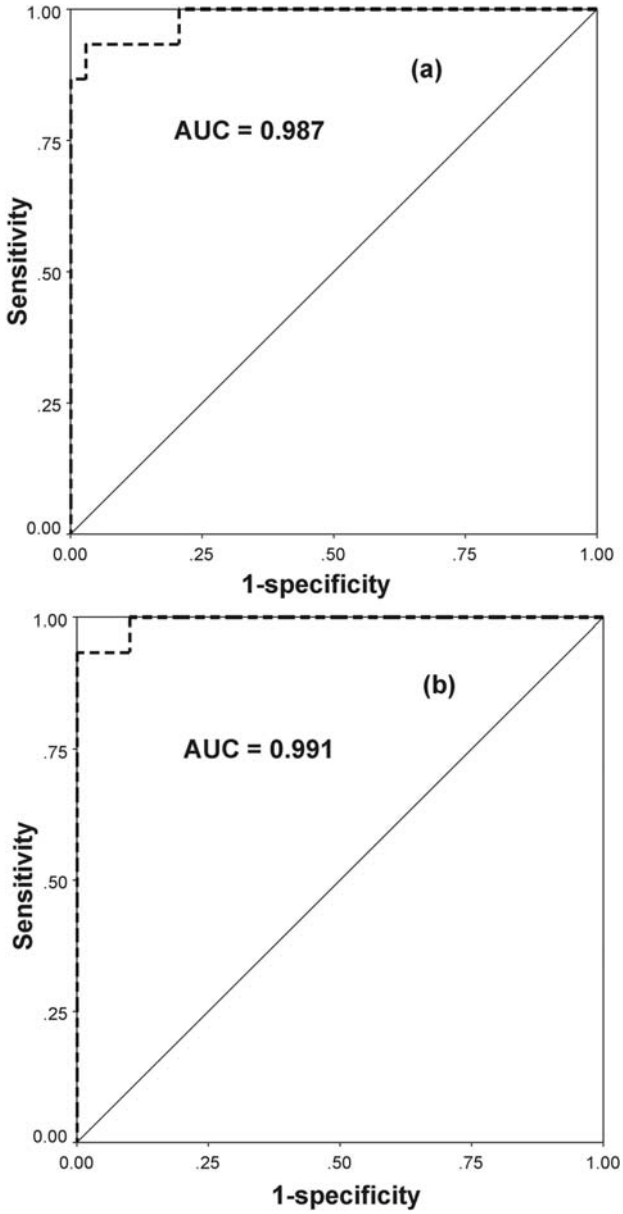

Figure 7 ROC curves showing the diagnostic performance of discriminant function scores for discriminating non-malignant from malignant oral lesions, (**a**) AF technique, and (**b**) DR technique.

mouth (FM) (Figure 3a), and ventral tongue (VT) (Figure 4a) indicates alterations in both the epithelium and stroma. The contributing factors to this reduction in fluorescence intensity are the breakdown of collagen crosslinks in the stroma, thickening of the epithelium, increased epithelial scattering, loss of keratin in the epithelium, and increased hemoglobin absorption associated with increased microvascular density throughout the epithelial-stromal region [1, 18, 19]. The redshift of the AF emission at 500 nm observed during tissue transformation towards malignancy is associated with the loss of fluorophores that emit at shorter wavelengths, such as NADH and FAD and the increase in relative contribution from porphyrins.

DR spectral features mainly depend on the absorption and scattering properties of tissues and on oxygenation levels of hemoglobin [7, 20]. Increased absorption at thickened epithelium, local architectural changes in the cellular and subcellular levels including changes in the nuclear to cytoplasmic ratio of the epithelial cells, stromal properties and neovascularization contribute to the decrease in reflectance intensity with abnormality [21, 22]. The DR spectral intensity at 545 and 575 nm in BM, FM and VT (Figures 2b, 3b and 4b) were found decreasing with in-

Table 2. Diagnostic accuracies obtained using autofluorescence (AF) and diffuse reflectance (DR) spectral methods.

Diagnostic accuracies	Normal (30) Vs Hyperplasia (15)		Dysplasia (26) Vs SCC (24)		Hyperplasia (15) Vs dysplasia (26)	
	Sensitivity	Specificity	Sensitivity	Specificity	Sensitivity	Specificity
AF	100%	93%	92%	100%	96%	92%
DR	100%	100%	100%	93%	100%	96%

Number of sites examined is given in parenthesis.

crease in malignancy (Table 3). This could be due to a reduction in production of oxygenated hemoglobin in the diseased regions. It has been reported that heme production via Heme cycle weakens in cancer cells due to a reduction in ferrochelatase activity [10, 19]. The diagnostic accuracies obtained for the AF and DR techniques (Table 2) based on the comparison of the scatterplots of discriminant function scores (Figures 5 and 6) with the pathological reports show the efficacy of these techniques in a clinical environment.

In vivo DR and AF spectroscopy have been applied for distinguishing benign and premalignant tissues in various organs. Georgakoudi et al. [20] and others have proposed a method called trimodal spectroscopy in which diffuse reflectance, autofluorescence and light-scattering spectroscopy were used simultaneously for tissue diagnosis. In this method, diffuse reflectance and autofluorescence spectra were measured, and two models were applied to extract intrinsic autofluorescence spectra and light scattering spectra. Studies performed for Barrett's esophagus (16 patients) and the cervix (44 patients) gave higher sensitivities and specificities for the combined methods than for any of the methods separately [23]. In a study using the same technique in 8 volunteers and 15 patients with oral lesions, a sensitivity of 96% and specificity of 96% was obtained for distinguishing lesions from healthy mucosa [1].

Lin et al. [24] compared in vivo AF and DR spectra from brain tumors and normal brain tissue. A two-step algorithm based on fluorescence and DR intensity at 460 nm produced a sensitivity of 89% and specificity of 76% for distinguishing tumor-bearing brain tissue from normal. Nordstrom et al. measured AF and DR spectra from the cervix and applied multivariate analysis and obtained sensitivities of 86–91% and specificities of 87–93% for distinguishing cervical intraepithelial lesions from normal squamous tissues using AF [25]. However, metaplasia (benign) and cervical intraepithelial lesions could not be separated. For DR, the diagnostic accuracies for distinguishing cervical intraepithelial neoplasia (CIN) from normal tissue were lower, but the classification of metaplastic versus dysplastic lesions was more successful (sensitivity of 77% and specificity of 76%).

As compared to these reports, using AF we have obtained a sensitivity of 96% and a specificity of 92% to discriminate dysplasia from hyperplasia (Table 2) while using DR a sensitivity of 100% and specificity of 96% was attained. It may be noted that the major clinical challenge is to distinguish pre-cancerous/dysplatic lesion from mimicking bengin or hyperplastic lesions. In the case of AF, the spectrum from the dorsal/lateral sides of the tongue fails to detect malignant lesions due to bacterial emissions [26]. Therefore, the high diagnostic accuracies along with its suitability for monitoring all types of oral cavity lesions strongly advocates the applicability of DR technique is a clinical situation.

The diagnostic performance of AF and DR technique was calculated using area under the ROC curve. The ROC analysis with discriminant score yielded area under the curve (AUC) of 0.987 for fluorescence spectral data (Figure 7a) and 0.991 for DR spectral data (Figure 7b) in discriminating non-malignant (normal and hyperplasia) from malignant (dysplastic and SCC) oral lesions. In comparison De Veld et al. recorded AF and DR spectra from 172 oral lesions and 70 healthy volunteers and achieved ROC areas up to 0.90 for the classification

Table 3. Normalized DR intensity of oxygenated hemoglobin absorption at 545 and 575 nm for different lesions.

Tissue types	Buccal mucosa		Floor of the mouth		Ventral tongue	
	545 nm	575 nm	545 nm	575 nm	545 nm	575 nm
Normal	0.44 ± 0.05	0.56 ± 0.04	0.57 ± 0.03	0.67 ± 0.02	0.52 ± 0.04	0.64 ± 0.03
Hyperplasia	0.41 ± 0.02	0.51 ± 0.06	0.54 ± 0.02	0.64 ± 0.03	0.47 ± 0.00	0.59 ± 0.00
Dysplasia	0.39 ± 0.01	0.47 ± 0.03	0.53 ± 0.05	0.63 ± 0.07	0.46 ± 0.04	0.54 ± 0.05
SCC	0.36 ± 0.02	0.41 ± 0.04	0.38 ± 0.01	0.44 ± 0.06	0.32 ± 0.06	0.38 ± 0.03

of diseased lesions (including dysplastic and cancerous) versus healthy mucosa for both AF and DR, and found classification of benign and pre-malignant lesions difficult (ROC areas <0.70 for AF and ROC areas up to 0.77 for DR) [4].

The AUC is a measure of the accuracy of a diagnostic procedure and the closer the AUC value is to 1.0 or 100%, the better is the accuracy of the procedure. In this comparative study the AUC for both AF and DR measurements show similar accuracies and can be considered useful in a clinical situation for detection and classification of oral cancer.

5. Conclusions

In this paper, we have explored and compared the potential utility of AF and DR for clinical screening of different oral lesions, such as leukoplakia, erythroplakia, ulcero proliferative growth, erosive lichen planus and SCC. Even though both AF and DR techniques offer better diagnostic accuracies for lesion discrimination, the DRS provides slightly improved classification accuracy as compared to AFS when evaluated on the same set of samples using similar analytical methods in this clinical study. Therefore, both these spectroscopic methods are applicable for clinical diagnosis of lesions of the oral cavity. However, DRS has the added advantage of discriminating all types of tissues of the oral cavity, including the tongue and lip that have poor diagnostic ability with autofluorescence technique.

Examination of lesions by point monitoring with a fiber-optic probe usually takes a long time when the lesion size is large. Improved diagnostic accuracies obtained in this trial support the clinical relevance of DR imaging in detection of the most malignant site in a lesion for biopsy, in lesion classification and in oral-cavity screening programs.

Acknowledgements This work was supported with grants from the Department of Science & Technology, Govt. of India [*SP/S2/L-19/1999*] and the Centre for Earth Science Studies Plan-223 project. JJL acknowledges Council of Scientific and Industrial Research (CSIR), New Delhi for her senior research fellowship.

Jayaraj L. Jayanthi was a researcher in the Biophotonics Laboratory of the Centre for Earth Science Studies (CESS), Akkulam, Trivandrum, and is presently working as Research Associate of the Department of Biotechnology, Govt. of India at the Regional Cancer Centre, Trivandrum. She has submitted her Ph.D. thesis and is awaiting the award of degree from the University of Kerala, Trivandrum. Her doctoral thesis is focused on autofluorescence and diffuse reflectance spectroscopy for non-invasive detection of oral cancer. Her research interests are in the areas of biomedical optics, cancerous lesion imaging, spectroscopic techniques in the diagnosis of oral and cervical cancer, and in cancer PDT.

Narayanan Subhash received his Masters in Physics from Kerala University, India, in 1975 and his Ph.D. in Laser Physics from the Cochin University of Science & Technology, India, in 1982. He was a Marie Curie Fellow of the European Union in 1993, a DAAD Fellow in 1998, and a Regular Associate of the International Centre for Theoretical Physics, Trieste, Italy during 1992–1999. He works as a Senior Scientist leading the Atmospheric Sciences Division at the Centre for Earth Science Studies, Trivandrum and is in charge of the Biophotonics R&D activities of the Centre. His current research interests are cancer diagnostics using point monitoring and multi-spectral imaging, detection of periodontal infections using optical spectroscopy, antimicrobial and cancer PDT, coral stress detection using laser-induced fluorescence, and sunlight-induced fluorescence imaging of vegetation.

Manju Stephen is an MDS from Kerala University and a Senior Resident in Oral and Maxillofacial Pathology Department at Govt. Dental College, Trivandrum. Her MDS thesis was focused on the diffuse reflectance imaging for the early detection of malignant changes in the oral cavity. Her current research interests are in oral pathology and DR imaging for medical applications.

Philip E. Kolady has completed his MDS from Kerala University and is presently working as a Senior Resident in the Department of Oral and Maxillofacial Pathology at Govt. Dental College, Kottayam, India. His MDS thesis focuses on spectroscopic diagnosis of early malignant changes in the oral cavity. His scientific interests are in the field of detecting dysplasia in pre-malignant oral lesions using autofluorescence and diffuse reflectance spectroscopy.

Valappil T. Beena is Professor and Head of the Department of Oral and Maxillofacial Pathology in the Govt. Dental College, Trivandrum. Her research interests include pathology of oral cancers and precancers, and spectroscopic detection of oral cancer.

References

[1] G. M. Muller, T. A. Valdez, I. Georgakoudi, V. Backman, C. Fuentes, S. Kabani, N. Laver, Z. Wang, C. W. Boone, R. R. Dasari, S. M. Shapshay, and M. S. Feld, Cancer **97**, 1681–92 (2003).
[2] F. P. Catherine, N. Samson, W. B. Kenneth, P. M. Williams, P. R. Miriam, and L. Zhang, J. Can. Dent. Assoc. **74**(3), 283–288 (2008).
[3] I. J. Bigio and S. G. Bown, Cancer Biol. Therapy **3**(3), 259–267 (2004).
[4] D. C. G. De Veld, M. Skurichina, M. J. H. Witjes, R. P. W. Duin, H. J. C. M. Sterenborg, and J. L. N. Roodenburg, Laser Surg. Med. **36**(5), 356–364 (2005).
[5] G. A. Wagnieres, W. M. Star, and B. C. Wilson, Photochem. Photobiol. **68**, 603–632 (1998).
[6] S. A. Boppart, T. F. Deutsch, and D. W. Rattner, Surg. Endosc. **13**, 718–722, (1999).
[7] R. A. Schwarz, W. Gao, C. Redden Weber, C. Kurachi, J. J. Lee, A. K. El-Naggar, R. Richards-Kortum, and A. M. Gillenwater, Cancer **115**(8), 1669–79 (2009).
[8] J. R. Mourant, I. J. Bigio, J. Boyer, R. L. Conn, T. Johnson, and T. Shimada, Laser Surg. Med. **17**, 350–357 (1995).
[9] C. Zhu and G. M. Palmer, Laser Surg. Med. **38**, 714–724 (2006).
[10] R. Mallia, S. S. Thomas, A. Mathews, R. Kumar, P. Sebastian, J. Madhavan, and N. Subhash, J. Biomed. Opt. **13**(4), 041306 (1–9) (2008).
[11] N. Ramanujam, M. F. Mitchell, M. Anitha, T. Sharon, A. Neely, and R. Richards-Kortum, Laser Surg. Med. **19**, 63–74 (1996).
[12] C. Y. Wang, T. Tasi H. M. Chen, C. T. Chen, and C. P. Chiang, Laser Surg. Med. **32**, 318–326 (2003).
[13] S. D. Kamath and K. K. Mahato, J. Biomed. Opt. **12**(1), 014028 (1–9) (2007).
[14] R. J. Mallia, S. S. Thomas, A. Mathews, R. Kumar, P. Sebastian, J. Madhavan, and N. Subhash, Cancer **112**, 1503–1512 (2008).
[15] D. C. G. De Veld, M. Skurichina, M. J. H. Witjes, R. P. W. Duin, H. J. C. M. Sterenborg, W. M. Star, and J. L. N. Roodenberg, Laser Surg. Med. **32**(5), 367–376 (2003).
[16] J. L. Jayanthi, R. J. Mallia, S. T. Shiny, K. V. Baiju, M. Anitha, K. Rejnish, S. Paul, M. Jayaprakash, G. N. Aparna, and N. Subhah, Laser Surg. Med. **41**, 345–352 (2009).
[17] J. L. Jayanthi, U. Nisha, S.Manju, E. K. Philip, P. Jeemon, K. V. Baiju, V. T. Beena and N. Subhash, BMJ Open July 2011 [doi:10.1136/bmjopen-2011-000071].
[18] U. Gustafsson, E. McLaughlin, E. Jacobson, J. Hakansson, P. Troy, M. Deweert, S. Palsson, M. S. Thompson, S. Svanberg, A. Vaitkuviene, and K. Svanberg, Proc. SPIE **5031**, 52–530 (2003).
[19] R. A. Schwarz, W. Gao, D. Daye, M. D. Williams, R. Richards-Kortum, and A. M. Gillenwater, Appl. Optics **47**(6), 825–834 (2008).
[20] J. W. Tunnell, A. S. Haka, S. A. McGee, Mirkovic and M. S. Feld, Tech. Gastrointest. Endosc. **5**(2), 65–73 (2003).
[21] I. Georgakoudi, E. E. Sheets, M. G. Muller, V. Backman, C. P. Crum, K. Badizadegan, R. R. Dasari, and M. S. Feld, Am. J. Obstet. Gynecol. **186**, 374–82 (2002).
[22] K. Badizadegan, V. Backman, C. W. Boone, C. P. Crum, R. R. Dasari, I. Georgakoudi, K. Keefe, K. Munger, S. M. Shapshay, E. E. Sheets, and M. S. Feld, Faraday Discuss. **126**, 265–279 (2004).
[23] I. Georgakoudi, B. C. Jacobson, J. Van Dam, V. Backman, M. B. Wallace, M. G. Muller, Q. Zhang, K. Badizadegan, D. Sun, G. A. Thomas, L. T. Perelman, and M. S. Feld, Gastroenterology **120**, 1620–1629 (2001).
[24] W. C. Lin, S. A. Toms, M. Johnson, E. D. Jansen, and A. Mahadevan-Jansen, Photochem. Photobiol. **73**(4), 396–402 (2001).
[25] R. J. Nordstrom, L. Burke, J. M. Niloff, and J. F. Myrtle, Laser Surg. Med. **29**(2), 118–127 (2001).
[26] R. J. Mallia, N. Subhash, J. Madhavan, P. Sebastian, R. Kumar, A. Mathews, G. Thomas, and J. Radhakrishnan, Appl. Spectrosc. **64**(4), 409–418 (2010).